

The basal chromospheric Mg II $h+k$ flux of evolved stars: Probing the energy dissipation of giant chromospheres

M. Isabel Pérez Martínez¹, K.-P. Schröder^{1*}, and M. Cuntz²

¹*Departamento de Astronomía, Universidad de Guanajuato, A.P. 144, Guanajuato, GTO, C.P. 36000, Mexico*

²*Department of Physics, University of Texas at Arlington, Box 19059, Arlington, TX 76019, USA*

Accepted 2011; Received 18.07. 2010

ABSTRACT

Of a total of 177 cool G, K, and M giants and supergiants, we measured the Mg II $h+k$ line emission of extended chromospheres in high-resolution (LWR) IUE spectra by using the IUE final data archive at STScI, and derived the respective stellar surface fluxes. They represent the chromospheric radiative energy losses presumably related to basal heating by the dissipation of acoustic waves, plus a highly variable contribution due to magnetic activity.

Thanks to the large sample size, we find a very well-defined lower limit, the basal chromospheric Mg II $h+k$ line flux of cool giant chromospheres, as a function of T_{eff} . A total of 16 giants were observed several times, over a period of up to 20 years. Their respective minimal Mg II $h+k$ line fluxes confirm the basal flux limit very well because none of their emissions dip beneath the empirically deduced basal flux line representative for the overall sample. Based on a total of 15 to 22 objects with very low Mg II $h+k$ emission, we find as limit: $\log F_{\text{MgII}hk} = 7.33 \log T_{\text{eff}} - 21.75$ (cgs units; based on the $B - V$ relation). Within its uncertainties, this is almost the same relation as has been found in the past for the geometrically much thinner chromospheres of main sequence stars. But any residual dependence of the basal flux on the surface gravity is difficult to determine, since especially among the G-type giants there is a large spread of the individual chromospheric Mg II fluxes, apparently due to revived magnetic activity. However, it can be stated that over a gravity range of more than four orders of magnitude (main-sequence stars to supergiants), the basal flux does not appear to vary by more than a factor of 2.

These findings are in good agreement with the predictions by previous hydrodynamic models of acoustic wave propagation and energy dissipation, as well as with earlier empirical determinations. Finally, we also discuss the idea that the ample energy flux of the chromospheric acoustic waves in a cool giant may yield, as a by-product, the energy flux required by its cool wind (i.e., non-dust-driven, “Reimers-type” mass-loss), provided a dissipation mechanism of a sufficiently long range is operating.

Key words: Stars: chromospheres – Stars: late-type – Stars: mass-loss – Stars: supergiants – Stars: winds, outflows – Stars: activity

1 INTRODUCTION

The physical processes operating within the chromospheres of cool stars are very complex and are still far from being fully understood. The dissipation of chromospheric energy can be probed by the related radiative cooling via chromospheric line emission, most importantly the Mg II and Ca II lines, see Linsky & Ayres (1978). As discussed in more detail by Judge (1990), radiative cooling is not much affected by the optical thickness of the lines. The photons

leave from a low-density giant chromosphere after multiple line-scattering (“effectively thin”). Empirically, the chromospheric line emission shows a minimal, i.e., “basal” flux level, that depends on the effective temperature (Strassmeier et al. 1994; Schrijver 1987; Rutten et al. 1991), above which there is a wide distribution of line emissions for the different stars (Vilhu & Walter 1987), which also may vary with time.

It has been suggested to associate the basal flux with the dissipation of purely mechanical (i.e., acoustic wave) energy in the turbulent chromosphere (e.g., Buchholz, Ulmschneider & Cuntz 1998), while energy released by magnetic activity phenomena is expected to produce the wide variation

* email: kps@astro.ugto.mx

of emission beyond the basal flux. Albeit this is a simple picture, there is still a number of open questions remaining. Nevertheless, this view appears to be at least consistent with existing empirical evidence for chromospheric energy dissipation (e.g., Ulmschneider 1991; Cuntz, Ulmschneider & Musielak 1998; Cuntz et al. 1999; Theurer, Ulmschneider & Kalkofen 1997; Fawzy et al. 2002; see also review by Musielak 2004). Specifically, a similar dependence on the effective temperature is obtained ($\propto T_{\text{eff}}^{7..8}$; see Musielak & Rosner 1988 and Buchholz et al. 1998, particularly their Fig. 15) for both the initial acoustic wave energy flux and the radiative emission flux observed as basal emission. Furthermore, acoustic wave dissipation is mostly independent of gravity (see Ulmschneider 1988, 1989 and Cuntz, Ramacher & Ulmschneider 1994), providing a further empirical prediction that can be tested by observation.

While earlier studies (e.g., Strassmeier et al. 1994) have already established that the basal flux emission declines towards cooler stars with a large power of T_{eff} , this type of work was mostly based on main-sequence (MS) stars. In contrast, our focus is on the basal flux emission of low-gravity stars; i.e., stars with about two (giants LC III) to over four orders of magnitude (supergiants LC I) lower surface gravity than the Sun. Hence, we not only aim at refining the dependence of the basal flux on T_{eff} , but also at contesting any possible dependence of the basal flux on gravity.

Giant stars also present an interesting case, noting that only a small fraction of their chromospheric mechanical flux would be needed to satisfy the input requirements of their non-dust-driven (“Reimers-type”) cool winds, assuming that a mechanism with a sufficiently large dissipation length operates (e.g., Holzer & MacGregor 1985; Cuntz 1990; Sutmman & Cuntz 1995). Schröder & Cuntz (2005) have shown, based on a simple analysis of the energy requirements of the winds, that such a mechanism would be well consistent with the Reimers formula (Reimers 1977). The resulting, improved mass loss relation was then successfully tested by Schröder & Cuntz (2007). An updated concept of structured red giant chromospheres and winds initiated by magnetized hot bubbles and the action of Alfvén waves, including long-range action by mode-coupling, has been given by Suzuki (2007). His models are also consistent with the existence of a small hot gas component apparently buried under a large column of chromospheric material (Ayres, Brown & Harper 2003).

To revisit the empirical evidence, we measure the chromospheric emission line fluxes of 177 giant and supergiant stars (Sect. 2). Thereafter, we determine the basal emission flux for this sample, including its dependence on T_{eff} (Sect. 3), by a detailed statistical analysis. We also take a look at how well the observed variability of 19 stars over periods of up to two decades is consistent with the basal flux concept. As we find no evidence for a significant dependency on gravity, we derive an upper limit to any residual change of basal flux over a gravity range of 4 orders of magnitude. Associated aspects of stellar evolution are elucidated in Sect. 4. Finally, we compare our results with previous empirical and theoretical findings (Sect. 5) and present our discussion and conclusions (Sect. 6).

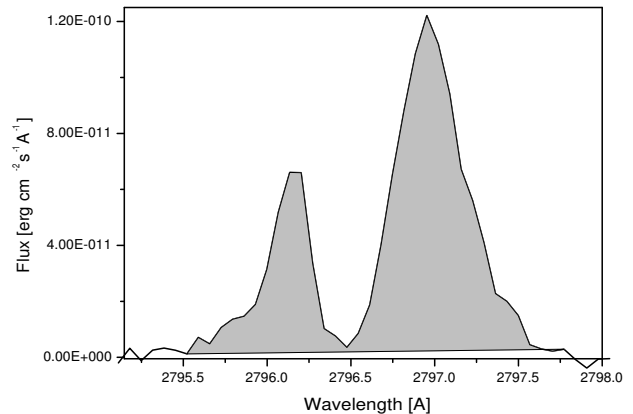


Figure 1. Mg II k chromospheric emission line: the shaded area shows the range considered for the flux integration.

2 DERIVING THE MG II $h+k$ CHROMOSPHERIC EMISSION LINE SURFACE FLUX

2.1 Measurements of the Mg II $h+k$ chromospheric emission using the IUE final data archive

The Mg II lines, representing a transition to the Mg II ground level, form a strong doublet, denoted as Mg II h (2803 Å) and Mg II k (2796 Å), respectively. For our measurements of the chromospheric Mg II emission line fluxes, only well-exposed spectra taken in the high resolution mode are suitable. There is a substantial body of previous work on the Mg II emission in late-type giants and supergiants. Examples include papers by Stencel et al. (1980), Simon & Drake (1989), Dupree, Hartmann & Smith (1990) and Peterson & Schrijver (1997). These authors obtained and analyzed IUE spectra for various samples of evolved stars, including metal-deficient stars. For many of these stars, they were able to identify asymmetric Mg II profiles, which were considered a unique signature of differentially expanding atmospheres due to the presence of outward mass motions. In the view of the evolutionary status of these stars, the authors often attribute this finding to the action of hydrodynamic processes, i.e., acoustic or pulsational waves; see, e.g., discussion by Dupree et al. (1990).

The final IUE data archive (Nichols & Linsky 1996; Nichols 1998) is, thanks to the 19 years of record-lifetime of the venerable IUE satellite (i.e., IUE accomplished over 100,000 observations between 1978 to 1996), even today a highly valuable data base, especially for stellar research. IUE spectra have, in their high-resolution mode, a spectral resolution of 20,000 and cover the wavelength range of 3400 to 1150 Å. IUE had two individual echelle spectrographs equipped with two cameras each, the primary (P) and redundant (R) cameras. Spectra of the longer wavelength range (LW), which included the chromospheric Mg II doublet, were taken by the LWR or the LWP camera.

For our study, we consider Mg II $h+k$ IUE observations for a total of 177 cool giants and supergiants of spectral

Table 1. Physical and empirical surface fluxes of the chromospheric Mg II $h+k$ line emission of 190 cool giants and supergiants from the IUE final data archive, together with $B - V$, V , BC and $\log T_{\text{eff}}$ (see Sect. 2). Stars with a minimum flux obtained from several observations are marked by an asterisk (*). Stars used to determine the basal flux line using the $B - V$ color transformation are marked by a dagger (†), whereas stars associated with the $V - K$ color transformation are marked by a double dagger (‡).

HD	$B - V$	$V - K$	$F_{\text{MgII}hk}$	BC_V	BC_K	$\log T_{\text{eff}}$	$\log T_{\text{eff}}$	$\log F_{\text{MgII}hk}$	$\log F_{\text{MgII}hk}$
...	from $B - V$	from $V - K$	from $B - V$	from $V - K$
28	1.02	2.59	4.06E-12	-0.40	2.17	3.682	3.657	5.37	5.25
352	1.27	3.02	1.18E-11	-0.71	2.36	3.640	3.627	6.17	6.03
496 †	1.00	2.22	6.43E-12	-0.38	1.94	3.685	3.690	5.30	5.34
1522	1.19	2.45	9.39E-12	-0.60	2.09	3.653	3.668	5.12	5.24
2261	1.08	2.54	3.80E-11	-0.47	2.14	3.672	3.660	5.39	5.36
3627	1.26	2.77	1.15E-11	-0.69	2.26	3.642	3.643	5.01	5.07
3712	1.15	2.48	3.03E-11	-0.55	2.11	3.660	3.665	5.15	5.22
4128	1.01	2.29	1.02E-10	-0.39	1.99	3.684	3.683	5.75	5.78
4174	1.40	3.99	3.69E-12	-0.92	2.65	3.618	3.586	5.89	5.35
4502	1.08	2.46	8.30E-11	-0.48	2.10	3.670	3.667	6.39	6.40
6805 †	1.15	2.51	8.70E-12	-0.55	2.12	3.660	3.663	5.09	5.16
6860	1.56	3.86	7.89E-11	-1.35	2.62	3.587	3.590	4.88	4.92
8512 †	1.05	2.28	7.59E-12	-0.45	1.98	3.675	3.684	5.19	5.27
9053	1.52	3.84	3.68E-11	-1.21	2.61	3.596	3.590	5.18	5.12
9746	1.20	3.17	3.75E-11	-0.61	2.42	3.652	3.619	6.76	6.53
9927	1.26	2.89	7.51E-12	-0.69	2.31	3.642	3.635	4.95	4.95
10380	1.31	2.99	5.98E-12	-0.78	2.35	3.632	3.629	5.12	5.13
12929	1.14	2.77	4.54E-11	-0.55	2.26	3.660	3.643	5.23	5.17
13480	0.74	2.19	2.37E-11	-0.15	1.92	3.736	3.693	6.58	6.33
17506	1.56	3.24	1.47E-11	-1.33	2.44	3.589	3.616	4.85	5.02
18322	1.07	2.38	8.02E-12	-0.47	2.05	3.672	3.674	5.31	5.36
18884	1.61	4.30	4.59E-11	-1.60	2.71	3.574	3.576	4.69	4.67
19476	0.97	2.52	8.08E-12	-0.35	2.13	3.690	3.662	5.39	5.25
20644 † ‡	1.49	3.41	3.30E-12	-1.15	2.50	3.600	3.608	4.60	4.65
20720	1.59	4.75	2.68E-11	-1.49	2.79	3.579	3.565	4.98	4.71
23817 †	1.12	2.53	6.76E-12	-0.53	2.14	3.663	3.661	5.16	5.19
24512	1.57	4.23	3.09E-11	-1.39	2.70	3.585	3.578	4.93	4.82
25025	1.57	3.86	2.72E-11	-1.39	2.62	3.585	3.590	4.75	4.81
26967	1.07	2.58	6.62E-12	-0.47	2.17	3.672	3.657	5.21	5.16
27371	0.97	2.09	1.03E-10	-0.35	1.84	3.690	3.705	6.44	6.52
27697	0.97	2.08	1.05E-11	-0.35	1.84	3.690	3.705	5.50	5.58
28305	1.00	2.06	9.69E-12	-0.38	1.82	3.685	3.708	5.34	5.47
28307	0.94	2.15	1.78E-11	-0.32	1.89	3.696	3.697	5.79	5.81
29139 *	1.53	3.90	1.70E-10	-1.28	2.63	3.592	3.589	4.79	4.77
31398 *	1.44	3.39	3.06E-11	-0.94	2.49	3.616	3.609	5.00	4.93
31767 † ‡	1.27	2.86	3.42E-12	-0.66	2.30	3.646	3.637	4.99	4.89
32068	1.08	3.26	6.14E-11	-0.40	2.45	3.682	3.615	6.18	5.66
32887	1.44	3.33	1.70E-11	-1.00	2.47	3.611	3.611	4.90	4.93
32918	0.98	2.51	4.87E-12	-0.37	2.12	3.687	3.663	6.86	6.65
37160	0.94	2.25	9.57E-12	-0.32	1.96	3.696	3.687	5.62	5.59
39364	0.97	2.32	1.27E-11	-0.36	2.01	3.689	3.680	5.57	5.54
39425	1.14	2.41	1.50E-11	-0.54	2.06	3.662	3.672	5.20	5.32
39801 * ‡	1.46	4.71	3.02E-10	-0.99	2.78	3.612	3.565	5.06	4.45
40239	1.62	4.88	1.39E-11	-1.66	2.81	3.570	3.562	4.83	4.54
40409	1.01	2.32	3.11E-12	-0.40	2.01	3.682	3.680	5.27	5.29
42995	1.57	4.94	4.48E-11	-1.39	2.82	3.585	3.560	5.11	4.68
43039	1.00	2.56	5.89E-12	-0.39	2.15	3.684	3.659	5.43	5.30
44478 ‡	1.60	4.67	3.22E-11	-1.54	2.78	3.577	3.566	4.70	4.49
46697	1.09	2.54	2.41E-12	-0.48	2.14	3.670	3.660	6.28	6.21
47205	1.03	2.37	9.01E-12	-0.43	2.04	3.678	3.675	5.43	5.45
50310 †	1.19	2.55	1.50E-11	-0.60	2.15	3.653	3.659	5.08	5.16
50877	1.54	3.03	9.78E-12	-1.28	2.37	3.591	3.627	4.75	4.92
52877	1.61	3.57	3.14E-11	-1.60	2.54	3.574	3.601	4.90	5.10
54810	1.00	2.41	3.77E-12	-0.38	2.06	3.685	3.672	5.48	5.42
56855	1.51	3.40	3.81E-11	-1.13	2.49	3.601	3.608	4.97	4.96
57669	1.18	2.60	1.71E-11	-0.59	2.18	3.655	3.655	6.06	6.04
59693 *	0.87	2.14	5.56E-12	-0.21	1.88	3.719	3.699	6.61	6.26
59717	1.49	3.48	1.30E-11	-1.15	2.52	3.600	3.605	4.70	4.78
60414	1.03	3.82	3.93E-10	-0.36	2.61	3.689	3.591	7.48	6.38
61772 † ‡	1.48	3.46	2.10E-12	-1.10	2.51	3.604	3.606	4.64	4.63

HD	$B - V$	$V - K$	$F_{\text{MgII}hk}$	BC_V	BC_K	$\log T_{\text{eff}}$ from $B - V$	$\log T_{\text{eff}}$ from $V - K$	$\log F_{\text{MgII}hk}$ from $B - V$	$\log F_{\text{MgII}hk}$ from $V - K$
...				
61935	1.01	2.26	5.95E-12	-0.39	1.97	3.684	3.686	5.28	5.31
62044 *	1.11	2.46	1.29E-10	-0.51	2.10	3.667	3.667	6.62	6.66
62345	0.92	2.00	9.18E-12	-0.30	1.77	3.699	3.716	5.42	5.49
62509 *	0.99	2.09	9.94E-11	-0.37	1.84	3.687	3.705	5.41	5.53
63032	1.57	3.59	2.24E-11	-1.37	2.55	3.586	3.600	4.94	4.98
63700 *	1.08	2.04	3.32E-11	-0.42	1.80	3.680	3.711	5.76	5.81
69267	1.45	3.26	1.35E-11	-1.05	2.45	3.608	3.615	4.90	5.00
71369 † ‡	0.84	1.96	1.04E-11	-0.23	1.73	3.715	3.721	5.47	5.48
73974	0.87	1.96	1.44E-12	-0.26	1.73	3.709	3.721	6.00	5.96
76294	0.96	2.37	1.31E-11	-0.35	2.04	3.690	3.675	5.33	5.26
77912	0.97	1.97	9.19E-12	-0.30	1.74	3.700	3.720	5.82	5.85
78647	1.61	3.78	1.01E-10	-1.60	2.60	3.574	3.593	4.90	5.08
80493	1.53	3.73	2.25E-11	-1.24	2.59	3.594	3.594	4.84	4.85
81797 †	1.42	3.07	3.93E-11	-0.98	2.38	3.613	3.625	4.80	4.95
81817	1.38	3.20	6.33E-12	-0.84	2.43	3.626	3.618	5.03	4.91
82210	0.77	2.00	3.05E-11	-0.18	1.77	3.727	3.716	6.48	6.41
82668 †	1.51	3.56	1.48E-11	-1.21	2.54	3.596	3.601	4.68	4.75
84441	0.78	1.68	3.73E-11	-0.19	1.43	3.725	3.766	5.93	6.05
85503	1.21	2.48	8.19E-12	-0.63	2.11	3.650	3.665	5.16	5.31
88284 ‡	1.00	2.05	6.14E-12	-0.38	1.81	3.685	3.709	5.17	5.31
89388	1.47	3.13	2.41E-11	-1.02	2.40	3.610	3.621	5.12	5.20
89484	1.12	2.78	4.07E-11	-0.52	2.26	3.665	3.642	5.22	5.11
89758	1.58	4.00	3.42E-11	-1.44	2.65	3.582	3.585	4.86	4.88
90610	1.39	3.19	6.80E-12	-0.92	2.43	3.618	3.618	5.00	5.02
93497	0.89	2.04	8.41E-11	-0.28	1.80	3.705	3.711	6.06	6.08
93813	1.22	2.82	1.56E-11	-0.64	2.28	3.648	3.640	5.12	5.11
94264	1.03	2.23	3.22E-12	-0.43	1.95	3.678	3.689	4.92	5.01
95272	1.06	2.30	5.79E-12	-0.46	2.00	3.673	3.682	5.25	5.33
95689 ‡	1.05	2.60	3.64E-11	-0.44	2.18	3.677	3.655	5.17	5.07
96833 † ‡	1.13	2.53	1.11E-11	-0.53	2.14	3.663	3.661	5.04	5.07
98262	1.36	3.09	1.59E-11	-0.79	2.39	3.631	3.624	5.16	5.11
98430	1.09	2.64	1.17E-11	-0.49	2.20	3.668	3.652	5.32	5.25
102350	0.85	1.74	1.02E-11	-0.25	1.50	3.711	3.756	5.74	5.88
104979 †	0.95	2.06	5.11E-12	-0.34	1.82	3.692	3.709	5.34	5.43
106677	1.10	2.56	1.59E-11	-0.51	2.15	3.667	3.659	6.53	6.49
107328	1.14	2.83	4.60E-12	-0.55	2.28	3.660	3.640	5.42	5.31
107446	1.37	3.22	1.11E-11	-0.87	2.44	3.623	3.617	4.98	4.96
108903 *	1.59	4.82	1.33E-10	-1.54	2.80	3.577	3.563	4.80	4.54
108907 *	1.56	4.40	6.26E-12	-1.39	2.73	3.585	3.573	4.93	4.71
109379 † ‡	0.88	1.89	2.36E-11	-0.27	1.67	3.707	3.731	5.50	5.60
111812	0.65	1.58	1.39E-11	-0.10	1.30	3.755	3.785	6.45	6.46
112300	1.55	4.52	2.45E-11	-1.35	2.75	3.587	3.570	4.90	4.65
113226	0.92	2.16	2.17E-11	-0.31	1.90	3.698	3.697	5.49	5.50
113996	1.45	3.22	3.36E-12	-1.05	2.44	3.608	3.617	4.81	4.92
115659 † ‡	0.91	1.93	1.62E-11	-0.30	1.70	3.701	3.726	5.44	5.55
116204	1.12	2.83	8.19E-12	-0.53	2.28	3.663	3.639	6.63	6.49
123139	1.00	2.32	3.48E-11	-0.39	2.01	3.684	3.680	5.29	5.31
124897 *	1.24	2.85	5.06E-10	-0.67	2.29	3.645	3.638	5.35	5.36
127665	1.28	2.77	1.03E-11	-0.74	2.26	3.637	3.643	5.04	5.14
127700	1.40	3.34	7.37E-12	-0.92	2.48	3.618	3.611	5.02	4.98
129078	1.39	3.06	3.96E-12	-0.92	2.38	3.618	3.625	4.59	4.66
129456 † ‡	1.34	3.22	5.00E-12	-0.81	2.44	3.628	3.617	4.86	4.80
131873	1.45	3.32	5.10E-11	-1.05	2.47	3.608	3.612	4.90	4.98
133208 † ‡	0.93	2.21	8.73E-12	-0.32	1.93	3.696	3.692	5.34	5.32
133216	1.65	4.57	3.49E-11	-1.89	2.76	3.560	3.569	4.68	4.71
134505 †	0.91	2.12	1.03E-11	-0.30	1.86	3.701	3.702	5.41	5.42
135722	0.95	2.20	1.23E-11	-0.33	1.93	3.694	3.692	5.47	5.47
137759	1.16	2.59	1.28E-11	-0.56	2.17	3.658	3.656	5.18	5.22
140573	1.16	2.46	1.94E-11	-0.56	2.10	3.658	3.667	5.10	5.20
141714	0.78	1.88	2.03E-11	-0.18	1.65	3.727	3.733	6.33	6.32
146051	1.57	3.86	3.71E-11	-1.39	2.62	3.585	3.590	4.79	4.86
146791	0.96	2.05	1.27E-11	-0.34	1.81	3.692	3.709	5.38	5.47
147675	0.91	2.09	2.18E-11	-0.30	1.85	3.701	3.704	5.92	5.93
148387 †	0.90	2.13	1.99E-11	-0.30	1.87	3.701	3.700	5.43	5.43

HD	$B - V$	$V - K$	$F_{\text{MgII}hk}$	BC_V	BC_K	$\log T_{\text{eff}}$ from $B - V$	$\log T_{\text{eff}}$ from $V - K$	$\log F_{\text{MgII}hk}$ from $B - V$	$\log F_{\text{MgII}hk}$ from $V - K$
...
148856	0.93	2.01	2.19E-11	-0.32	1.78	3.696	3.714	5.46	5.55
150798	1.41	2.97	9.08E-11	-0.88	2.34	3.622	3.630	5.21	5.30
150997 *	0.90	2.12	2.43E-11	-0.30	1.86	3.701	3.702	5.81	5.82
153210	1.15	2.44	1.21E-11	-0.56	2.08	3.658	3.669	5.11	5.23
153751	0.86	1.92	2.70E-11	-0.26	1.69	3.709	3.727	6.20	6.24
156283 ‡	1.40	3.08	1.23E-11	-0.88	2.39	3.622	3.624	4.84	4.88
157244	1.42	3.08	5.43E-11	-0.90	2.38	3.620	3.624	5.34	5.37
157999	1.36	2.92	7.51E-12	-0.80	2.32	3.630	3.634	5.16	5.13
159181 *	0.92	1.93	1.04E-10	-0.25	1.71	3.712	3.725	6.23	6.25
161096	1.16	2.30	1.76E-11	-0.56	2.00	3.658	3.682	5.11	5.30
161892	1.18	2.53	1.37E-11	-0.59	2.14	3.655	3.661	5.15	5.23
163588	1.17	2.65	9.24E-12	-0.58	2.20	3.657	3.651	5.20	5.22
163770 *	1.28	2.67	1.42E-11	-0.68	2.21	3.644	3.650	5.35	5.39
163993	0.92	2.17	2.20E-11	-0.31	1.91	3.698	3.695	5.84	5.83
167618	1.57	4.69	3.41E-11	-1.39	2.78	3.585	3.566	4.90	4.60
168723	0.93	2.16	1.22E-11	-0.32	1.90	3.696	3.696	5.38	5.40
169414	1.16	2.50	7.95E-12	-0.56	2.12	3.658	3.663	5.20	5.28
169916	1.02	2.47	2.01E-11	-0.40	2.10	3.682	3.666	5.35	5.29
171443 †	1.30	2.95	6.71E-12	-0.75	2.34	3.635	3.631	4.96	4.98
174974	1.23	2.42	9.19E-12	-0.59	2.08	3.654	3.670	5.64	5.59
177716	1.16	2.83	1.44E-11	-0.56	2.28	3.658	3.639	5.24	5.16
183492 † ‡	1.02	2.26	1.24E-12	-0.41	1.97	3.680	3.686	5.22	5.26
186791 *	1.46	3.31	3.90E-11	-1.02	2.47	3.610	3.612	5.06	5.09
187076	1.27	4.12	7.40E-11	-0.65	2.68	3.647	3.581	6.02	5.39
188650	0.62	1.25	3.20E-12	-0.08	0.70	3.764	3.874	6.20	6.28
188947	1.01	2.48	6.51E-12	-0.39	2.11	3.684	3.665	5.30	5.22
192876	0.86	2.18	1.48E-11	-0.21	1.91	3.721	3.694	6.04	5.84
196171	0.99	2.38	1.36E-11	-0.37	2.05	3.687	3.674	5.33	5.28
197989	1.01	2.47	2.68E-11	-0.40	2.10	3.682	3.666	5.34	5.28
198700	1.19	2.40	1.87E-11	-0.55	2.06	3.660	3.672	5.51	5.58
200905	1.49	3.43	2.09E-11	-1.10	2.50	3.604	3.607	5.13	5.08
202109 †	0.98	2.01	8.72E-12	-0.36	1.77	3.689	3.715	5.18	5.32
203387	0.87	2.01	1.98E-11	-0.26	1.78	3.709	3.714	6.09	6.10
204075	0.96	1.98	2.65E-11	-0.35	1.74	3.690	3.719	5.90	6.02
205435	0.87	2.04	2.58E-11	-0.27	1.81	3.707	3.710	6.07	6.09
205478	1.00	2.25	8.31E-12	-0.39	1.97	3.684	3.687	5.34	5.39
206778	1.45	3.05	9.58E-11	-0.99	2.38	3.612	3.626	5.34	5.44
206859	1.07	2.42	1.50E-11	-0.40	2.07	3.682	3.671	5.83	5.71
206952	1.09	2.78	2.10E-11	-0.49	2.26	3.668	3.643	5.97	5.84
207089	1.27	2.58	1.09E-11	-0.65	2.16	3.647	3.657	5.83	5.84
208816	0.72	2.78	3.32E-11	-0.12	2.26	3.747	3.643	6.85	5.35
209750 *	0.89	2.15	5.00E-11	-0.23	1.89	3.716	3.698	6.00	5.83
210745	1.49	2.84	3.07E-11	-1.07	2.29	3.606	3.638	5.19	5.44
211388	1.39	2.95	4.96E-12	-0.90	2.34	3.620	3.631	4.84	4.91
211416	1.37	3.19	1.76E-11	-0.88	2.43	3.622	3.618	6.28	4.89
213080	1.54	4.94	1.43E-11	-1.28	2.82	3.592	3.560	6.53	4.51
216228	1.04	2.19	1.02E-11	-0.44	1.92	3.677	3.693	6.47	5.41
216386	1.59	4.29	1.58E-11	-1.49	2.71	3.579	3.576	6.34	4.67
216489	1.10	2.52	4.17E-11	-0.51	2.13	3.667	3.662	8.00	6.77
217906	1.64	4.76	5.30E-11	-1.80	2.79	3.564	3.564	6.22	4.50
218356 *	1.23	2.85	4.86E-11	-0.67	2.29	3.645	3.638	7.57	6.21
219615	0.90	2.27	7.61E-12	-0.30	1.98	3.701	3.685	6.48	5.32
224427	1.54	4.57	7.40E-12	-1.31	2.76	3.589	3.569	6.44	4.57

types G, K, and M, encompassing the luminosity classes III to I, of which surface fluxes can be derived by the means described in Sect. 2.2. This heterogeneous stellar sample covers a conveniently wide, two-dimensional array of physical parameters (i.e., T_{eff} and g), as well as different evolutionary stages (see Sect. 4). A total of 16 objects have been observed several times and in many cases showed real variability. Mostly, the variability did not change the line profiles.

In cases of multiple observations, we focused on the lowest flux measurement for each star since it is expected to be closest to the basal flux, see Sect. 3.

The IUE database is available online from <http://archive.stsci.edu/iue/search.php>. Note that the photospheric UV flux in such cool stars is very low or virtually absent compared to the Mg II $h+k$ emission line peaks. This makes the magnesium doublet highly favourable

for chromospheric observational research. As mentioned above, another big advantage of the Mg II emission lines for chromospheric studies is that their peak emissivity, in essence, covers a wide range of the chromospheric temperature distribution. This not only invokes a very strong chromospheric emission line output, second only to the hydrogen lines, but even more importantly, the Mg II emission flux is able to serve as a universal probe of the chromospheric energy dissipation and radiative losses, as pointed out a long time ago (e.g., Linsky & Ayres 1978, see inset of their Fig. 1). Since the radiative cooling is still dominated by hydrogen, there is little, if any dependence of the Mg II line flux on metallicity (Cardini 2005).

Like most other chromospheric studies, our measurements were made for both Mg II $h+k$ lines. A simple integration over the line profile was made after subtracting the photospheric flux; see Fig. 1 for an example of Mg II k with the shaded area corresponding to the line integration. We also determined the photospheric flux at 2795.5 Å. This simple line integration procedure yields the physical emission line fluxes at Earth, $F_{\text{MgII-IUE}}$, for each of our sample stars (see Table 1). Stars, for which the lowest measurement was used from multiple observations, are marked with an asterisk (*). Stars used to determine the basal flux line through a statistical fitting procedure (see Sect. 3.1) are marked with a dagger (†) or double dagger (‡), respectively, depending on whether the $B - V$ or $V - K$ relation was employed for the color transformation (see Sect. 2.2).

2.2 Deriving Mg II emission line surface fluxes

A more difficult step consists in deriving the stellar chromospheric surface fluxes $F_{\text{MgII}hk}$. This could be done by directly using the distances and radii of the sample stars. In fact, direct parallax measurements are mostly quite accurate, i.e., almost 80% of the giants in our sample have a measurement error of only 10% or less of its parallax. However, the derivation of the radii still require the bolometric correction BC of each star. In this respect, direct determinations of the surface fluxes do not suffer any less from systematic errors than the various parallax-independent approaches, beginning with the Barnes-Evans relation for the visual surface brightness (Barnes, Evans & Moffett 1978). Deriving the angular diameters and, hence, the observed fluxes over surface flux ratios this way will depend on a color relation.

Here we use the relation by Oranje, Zwaan & Middekoop (1982) that uses BC

$$\log \frac{F}{f} = 0.35 + 4 \log T_{\text{eff}} + 0.4(V + BC) . \quad (1)$$

The constant 0.35 has been adjusted to be consistent with the revised solar quantities by Cox (2001).

The required values for T_{eff} , BC_V and BC_K were then derived from the color indices of each giant by the $B - V$ and $V - K$ color, using the color relations from Buzzoni et al. (2010):

$$B - V = 1.906 [BC_V^2 \exp(BC_V)]^{0.3} \quad (2)$$

$$BC_V = -\exp(27500 \text{ K}/T_{\text{eff}})/1000 \quad (3)$$

$$V - K = 1/(1 - 0.283 BC_K) \quad (4)$$

$$BC_K = -6.75 \log T_{\text{eff}}/9500 \text{ K} \quad (5)$$

We obtained the individual $V - K$ values from the Two Micron All Sky Survey (2MASS). The $V - K$ color index is considered to be much more temperature sensitive than the $B - V$ color, especially for evolved stars, but there is a trade-off: Extinction in $V - K$ reaches 91% of the visual interstellar absorption A_v (see Whittet & van Breda 1978), while $B - V$ is well known to amount only to 32% of A_v . For this reason, and for an appropriate comparison with historic work on the basal flux line, which relied mostly on $B - V$ color relations, we use here the $V - K$ derived data-set only for estimating the magnitude of the systematic errors (see below) inherent in the above relations.

Noting that our sample consists of giants stars, which typically are much more distant than main-sequence stars, interstellar absorption and extinction does become an issue. Hence, both color indices, $B - V$ and $V - K$, were individually corrected according to an average, distance-dependent interstellar absorption A_v of 1 mag per kpc. The distances were obtained from the parallaxes given by the Hipparcos catalogue. Of course, this correction only avoids systematic errors for the sample; however, it is not very accurate for the individual objects.

Figure 2 shows the derived chromospheric Mg II $h+k$ line emission surface fluxes of the 177 cool giants and supergiants obtained from the IUE archive, to which the above $B - V$ relation is applied, as a function of the effective temperature (see Sect. 3 and Table 1). Stars with multiple observations and clearly variable Mg II fluxes have been shown with their minimum fluxes. Thanks to the richness of the sample, the distribution of chromospheric fluxes shows, within some scatter, a lower limit with a simple dependence on T_{eff} (i.e., linear in double logarithmic representation).

3 THE BASAL CHROMOSPHERIC FLUX AS A FUNCTION OF T_{EFF}

3.1 Detailed statistical analysis

In order to gauge the significance of the line associated with the lower limits of the Mg II chromospheric emission fluxes (see Fig. 2), we pursue a detailed statistical analysis of the data. In principle, we distinguish between *systematic uncertainties* associated with the uncertainties of the individual data and *statistical uncertainties*, due to the uncertainty of the basal flux line itself (i.e., slope and y -axis intercept), associated with the spread of the observational data.

As data uncertainties, we take the estimated double amplitude of 20%, i.e., ± 0.04 in $\log F_{\text{MgII}hk}$. The value of 20% is essentially completely due to the F and f values (see Eq. 1), i.e., by the absolute flux measurements for Mg II $h+k$ and the conversion to the stellar surface fluxes. Physical quantities affecting the results include the visual magnitude of the star V , the bolometric correction BC as well as the adopted stellar distances and the stellar radii. A further small, almost negligible contribution to the systematic uncertainty arises from the subtraction of the stellar continuum from the flux measurements (see Fig. 1). This latter uncertainty is assumed to be negligible owing to the diminutive contribution of the the continuum to the measured Mg II h and k lines.

As part of our study, we deduced two different lines

Table 2. Statistical parameters of the basal flux line.

Model	N_*	A	σ_A	B	σ_B	R_{Sp}
$B - V$	22	-21.75	1.72	7.33	0.47	0.99995
$V - K$	15	-19.74	1.40	6.78	0.38	0.99989

for the lower limits of the Mg II fluxes in response to the usage of either the $B - V$ or $V - K$ relation for the color transformation (see Sect. 2.2). In the first case, the basal flux line is determined by using $N_* = 22$ stars, whereas in the second case $N_* = 15$ stars were used. The objects are listed in Table 1, noting that the selected objects for the two determinations are labelled by a dagger (\dagger) or double dagger (\ddagger), respectively.

The lines given in the form

$$\log F_{\text{MgII}hk} = B \log T_{\text{eff}} + A \quad (6)$$

are calculated by invoking a least-square fit with consideration of the uncertainty bar for its individual data point. In doing so, we used the statistical fitting procedure (SUBROUTINE FIT) as described by Press et al. (1986); see Table 2 for our results. This procedure also gives information on the uncertainty (i.e., standard deviation) concerning the slope (σ_B) and the y -axis intercept (σ_A).

For later depiction, we also calculated the interval estimates associated with the position of each basal flux line given by the sample (see greyish area); see, e.g., Montgomery, Peck & Vining (2006) for a brief description of the involved algebra. We considered both the systematic uncertainty of the data and the statistical uncertainty with respect to the two previously determined basal flux lines. We assumed a confidence interval (CI) of 95%, corresponding to 2.101 standard deviations. The systematic and the statistical uncertainties have been combined in a linear manner. The size of the uncertainties obtained for both A and B (see Table 2) are mostly due to the relative small number of objects considered for our analysis. Fortunately, however, they do not result in an overly large interval estimate for the position of either basal flux line.

A further result obtained by utilizing the procedure by Press et al. (1986) consists in the computation of the Spearman rank-order coefficient R_{Sp} (see Table 2) for the correlation between $\log F_{\text{MgII}hk}$ and $\log T_{\text{eff}}$. An outcome of -1 would indicate a perfect anti-correlation, whereas an outcome of $+1$ would indicate a perfect (positive) correlation. For the basal flux line obtained by employing the $B - V$ method, we obtain a R_{Sp} value of 0.99995, whereas for the basal flux line obtained by employing the $V - K$ method a R_{Sp} value of 0.99989 is found. Thus, in conclusion, there is an almost perfect (positive) correlation between $\log F_{\text{MgII}hk}$ and $\log T_{\text{eff}}$ for both lines, as expected.

Based on the above analysis, while noting that we prefer the $B - V$ based relation (see Sect. 2.2), the empirical basal flux of the full sample can be represented by a straight line given as

$$\log F_{\text{MgII}hk} = 7.33 \log T_{\text{eff}} - 21.75 \quad (7)$$

that is depicted in both Fig. 2 and Fig. 3. It is also depicted when comparing our results with previous empirical results

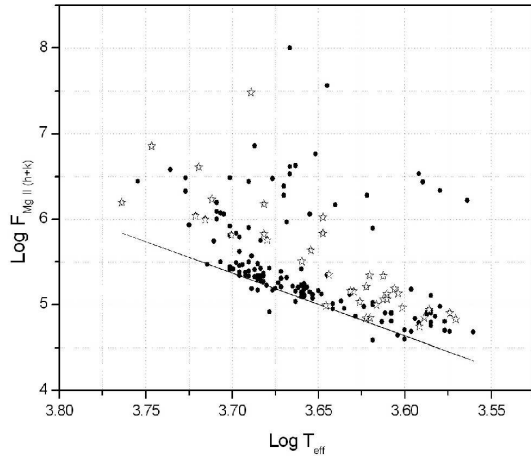


Figure 2. Measured Mg II $h+k$ chromospheric emission line surface fluxes of 177 giants as a function of T_{eff} based on a $B - V$ relation (see text for details). Open star symbols represent giants of LC I, dark dots LCs II and III. The straight line represents the derived basal flux.

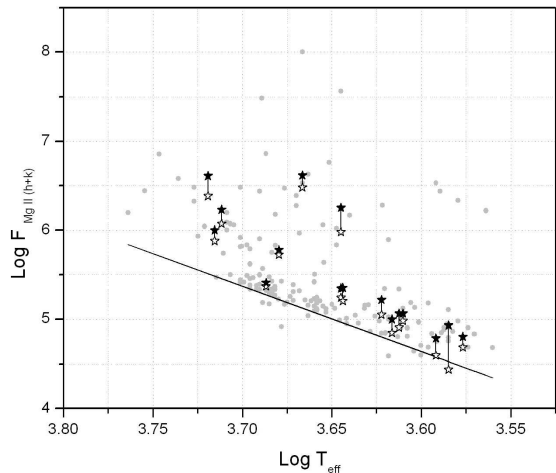


Figure 3. A plot of the 16 giants with multiple observations, showing both their average and their minimum Mg II $h+k$ fluxes, against the shaded backdrop of the total sample as in Fig. 2.

as well as results from detailed model computations (see Fig. 4).

Here, the statistical uncertainty of the empirical slope of the basal flux line in the $\log T_{\text{eff}} - \log F$ diagram, given as 7.33, is 0.47. The systematic errors are of similar order. When using the $V - K$ relations instead, the slope is 6.78, and if furthermore the Barnes-Evans relation is used for deriving the surface fluxes, with BC and T_{eff} taken from the $B - V$ relations above, the slope is 7.62. Hence, these alternative values fall on either side of the purely $B - V$ based result above.

3.2 Is stellar variability consistent with the basal flux limit?

Our sample consists of 16 giants and supergiants for which multiple observations exist (marked by an asterisk in Table 1) and to which the relations concerning the derivation of the Mg II fluxes (see Sect. 2.2) are applicable. In most cases, these observations span over at least several years, in some cases nearly the whole two decades of the IUE life time, a timescale comparable to the expected duration of long stellar activity cycles (e.g., Baliunas et al. 1995).

Hence, in view of all sporadic variations of stellar activity on timescales of months, as well as their systematic variations over the full activity cycle, the range of this variability should clearly lie above the basal flux limit. However, it should be noted that the large-scale of giant granular structure is also expected to yield a certain level of flux variation, expected to be statistical in nature, even in the case of pure acoustic wave heating (e.g., Judge & Cuntz 1993).

Figure 3 indicates that this is indeed the case concerning the 16 stars. It is noteworthy that, despite looking at 16 different objects over a relatively long period of time, *none* of them showed a minimum Mg II emission line flux dipping *below* the limit given by the basal chromospheric flux. Note that this assessment is valid for both basal flux limits obtained by employing either the $B - V$ or $V - K$ relationship; see Sect. 2.2.

3.3 Comparison with previous results

About the same temperature dependence as given above has been found in earlier studies (Oranje & Zwaan 1985; Schrijver 1987; Rutten et al. 1991), which were however mostly aimed at MS stars. For example, Rutten et al. (1991) derived a dependence on the effective temperature akin to T_{eff}^8 . A paper focused on the basal flux in G and K-type giants has been given by Strassmeier et al. (1994). They measured the Ca II line emission using ground-based spectroscopy. For the K-line they found a basal flux represented by

$$\log F_{\text{Ca II}} = 8 \log T_{\text{eff}} - 24.8, \quad (8)$$

which has a similar slope as the relationships obtained in our present study, particularly the relation based on $B - V$ color transformation (see Eq. 7).

A more recent result for the emission flux in Ca II was given by Pasquini, de Medeiros & Girardi (2000). They obtained Ca II H+K high resolution observations for 60 evolved stars of spectral type F to K located in five open clusters. Pasquini et al. (2000) found that the Ca II K fluxes scaled, in essence, linearly with the stellar rotational velocity, whereas the basal flux line scaled with respect to the stellar effective temperature according to $F_{\text{Ca I+K}} \propto T_{\text{eff}}^{7.7}$.

Hence, the slopes of the basal Mg II flux emission (based on $B - V$ and $V - K$ colors) as well as the slope of the previously derived basal Ca II flux emission fully agree with respect to each other within their respective uncertainties, if available. In absolute terms, the Mg II basal flux derived in the present study lies about 0.6 dex higher, while the expected off-set should be only about 0.3 dex due to the intrinsically smaller emission measure of the Ca II K lines compared to the Mg II lines, as well as other differences in the Ca II and Mg II line formation processes (for a de-

tailed study see, e.g., Linsky & Ayres 1978 and Ayres 1979). The remaining difference of a 0.3 dex higher basal flux deduced in the present study is attributable to the fact that the earlier work did not fully consider underlying uncertainties. The omission of uncertainties readily results in an artificially broadened flux distribution towards smaller values. If we choose not to average over various borderline cases (see Sect. 3.1) but simply set the basal flux line to consistently undercut *all* lowest flux values, our findings would essentially be in perfect agreement with the historical values.

4 STELLAR EVOLUTIONARY ASPECTS CONCERNING THE MG II EMISSION

Links to theoretical studies of angular momentum evolution have been explored by Gray (1991), Schrijver (1993), Schrijver & Pols (1993), Charbonneau, Schrijver & MacGregor (1997), and others. These studies show that when solar-type stars evolve away from the main-sequence, their rotation slows down beyond what must be expected from the increase in the moment of inertia caused by changes in the internal mass distribution. Hence, their angular momentum subsides, due to magnetic braking resulting from the onset of massive stellar winds. Thus, one would rather expect little magnetic activity in evolved stars. But as demonstrated by Fig. 2, this is mostly true only for M and late K giants (i.e., with $\log T_{\text{eff}} < 3.64$). By contrast, flux measurements for many G giants and G supergiants are spread over several orders of magnitude above their basal fluxes.

A look at the evolutionary history of the respective giants shows that the latter group should indeed be expected to exhibit strong magnetic activity, whereas the former should not. The same picture has been found empirically from the strength of coronal X-ray emission, and was explained based on the same reasoning (Schröder, Hünsch & Schmitt 1998): G giants are usually first-time Hertzsprung-gap crossers of about 1.5 to 2 M_{\odot} , whereas G supergiants are relatively massive (4 to 10 M_{\odot}) stars in their central He-burning phase. All these giants once were, as MS stars, too hot (i.e., spectral type earlier than F0) to possess convective outer layers; those only developed later. Hence, G giants and supergiants were unable to host a solar-like magnetic dynamo until only very recently in their evolutionary history, and their present magnetic activity has not suffered much from magnetic breaking.

By contrast, K and M giants have mostly evolved from less massive MS stars, as K giant clump stars and as RGB/AGB stars. Their progenitors have been active during their entire MS life times and suffered from magnetic breaking all along. Hence, for these stars, like in regards to their coronal X-ray emission, we find a reduced (but still not vanished) level of magnetic activity. It has therefore been argued (e.g., Dupree et al. 1990; Buchholz et al. 1998) that the dominant chromospheric heating mechanism in single inactive late-type (super-) giants might be essentially acoustic rather than magnetic in nature. Early results in support of this picture based on the analysis of the evolution of rotation rates and chromospheric activity of giants have been given by Rutten & Pylyser (1988).

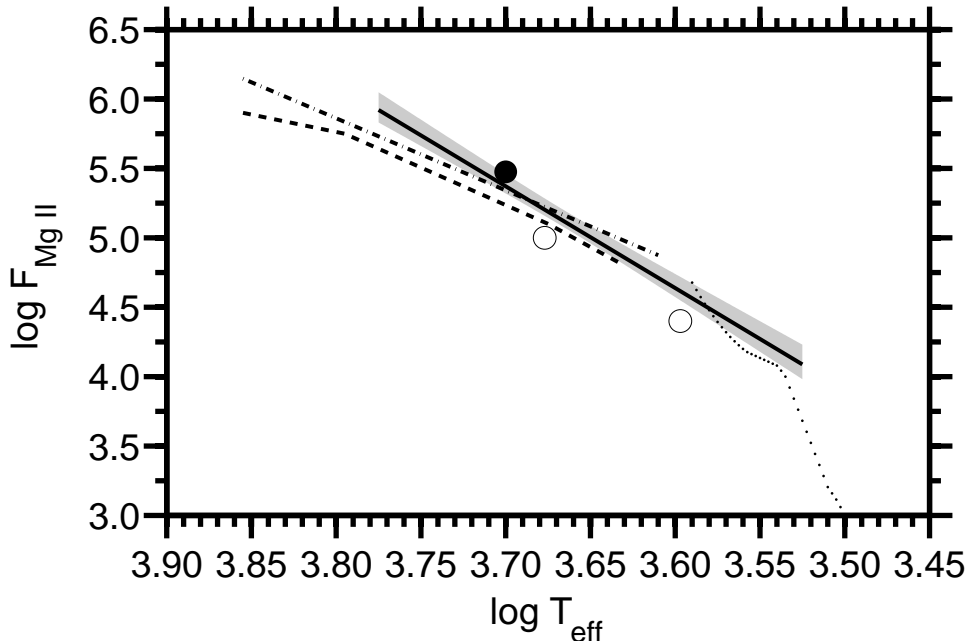


Figure 4. Diagram showing the basal flux limit for Mg II $h+k$ as a function of the stellar effective temperature obtained from $B - V$ colors (see Sect. 2) together with results from previous observations and theoretical simulations. The solid line shows our results for the object-selected basal flux line. The uncertainties due to statistical and systematic observational effects (see Sect. 3.4) are indicated by the greyish area. The dashed line shows the results from Rutten et al. (1991), whereas the dot-dashed line indicates the earlier results from Schrijver (1987). The dotted line shows the Mg II basal flux limit obtained through the sample by Judge & Stencel (1991). The circles represent results from previous theoretical simulations based on acoustic energy dissipation given by Cuntz et al. (1994) (closed circle) and Buchholz et al. (1998) (open circles).

5 COMPARISON WITH THEORETICAL STUDIES; POSSIBLE EFFECTS OF THE STELLAR SURFACE GRAVITY

Figure 4 offers a detailed comparison of our results for the chromospheric basal flux line with results from previous theoretical and empirical studies as given by Schrijver (1987), Rutten et al. (1991), Judge & Stencel (1991), Cuntz et al. (1994), and Buchholz et al. (1998). Even though the sample of stars presented here is much larger and has a different composition compared to some of the earlier studies, we find that our results are in good agreement, especially with the theoretical results obtained by Buchholz et al. (1998). With respect to the different approaches in the derivation of the chromospheric basal flux line and the associated systematic errors (see Sect. 3.1), no discernible differences were found. The systematic errors are commensurate to the uncertainties of the individual data.

As shown in Fig. 4, our observational results, i.e., the empirical basal flux limits for the adopted sample including the biparabolic envelopes for the associated statistical uncertainties, show considerable agreement with the previous results by Schrijver (1987) and Rutten et al. (1991). Agreement is found for the relatively hot segment of the sample ($T \gtrsim 4050$ K) with the previous results by Schrijver (1987) and Rutten et al. (1991) as well as for the relatively cool segment of the sample ($T \lesssim 3950$ K) with the result by Judge & Stencel (1991); note that none of these authors communicate any uncertainty bars for their results. Judge & Stencel provided an empirical analysis for the global thermodynamic properties of the outer atmospheres of giant stars

and a small number of supergiants by addressing both the mass-loss energetics and the outer atmospheric heating in the framework of previously proposed concepts.

Previous work by Linsky & Ayres (1978), Schrijver (1987) and Rutten et al. (1991) revealed the surprising property that the Ca II and Mg II basal flux lines for MS stars and giants essentially coincide. This result is, in principle, also consistent with the findings from the more recent study by Cardini (2005) based on 225 stars of luminosity class I to V, even though it is providing some indications that the Mg II k flux increases slowly (i.e., by a factor of 2) with decreasing stellar gravity, especially if supergiants are included. On the other hand, it is highly noteworthy that the targeted gravity range encompasses more than four orders of magnitude and, furthermore, a factor of 2 is well within one standard deviation of the position of the Mg II basal flux line obtained by the present study (see Fig. 4).

It has been suggested that the lack of a pronounced difference in the Mg II (and Ca II) basal flux limits is mainly caused by the enormous differences in the geometrical extent of the stellar radiative zones for the different types of stars, especially with respect to the H^- continuum (Ulmschneider 1988, 1989; Cuntz et al. 1994; Buchholz et al. 1998). In the framework of acoustic models, the wave energy flux at photospheric levels is significantly increased in giant stars compared to MS stars, but so is the extent and efficiency of the H^- radiative damping zones (Ulmschneider 1988, 1989). However, both features largely off-set each other, leading to a very similar amount of available wave energy in the Ca II and Mg II line formation region in MS and giant stars. Con-

sequently, for the special case of magnetically inactive stars, this behaviour can readily explain a relatively similar basal flux emission for both types of objects, consistent with observations. Cuntz et al. (1994) expanded this type of analysis to evolved stars of different metallicities which led to the same type of outcome, thus providing consistency with previous observational results by Dupree et al. (1990).

6 DISCUSSION AND CONCLUSIONS

With an unprecedented sample size and time coverage, our study confirms the concept of a basal chromospheric emission flux from a purely empirical point of view. We confirm a strong dependence of the flux on T_{eff} , while a dependence on gravity (shift of the basal flux regarding samples of stars of different luminosity classes) must be smaller than the involved statistical errors. In addition, all well documented cases of time-variable chromospheric flux emission (see Sect. 3.2, Fig. 3) remain well above the basal flux limit. We view this as further empirical evidence for a *physically different* origin of the basal flux, which is obviously unrelated to the highly time-variable heating processes associated with stellar magnetic activity.

We acknowledge that there is still an ongoing debate about the physical origin of the basal flux. Previously, Judge & Cuntz (1993) confronted the predictions of 1-D acoustic heating models for α Tauri (K5 III) with HST-GHRS observations. They arrived at a list of problems associated with the disagreements between the theoretical acoustic models and the observation. Judge & Cuntz (1993) concluded that α Tauri's chromosphere might either (partially) be magnetically heated or α Tauri has acoustic properties substantially different from those of traditional mixing-length models or its chromosphere is determined by 3-D turbulence and/or horizontal flows. However, so far, no detailed 3-D acoustic chromospheric heating models have been given for giant or supergiant stars, which would allow contesting the empirically deduced basal flux limits, although significant progress on the calculation of 3-D non-magnetic chromosphere models has meanwhile been made for the Sun (e.g., Wedemeyer et al. 2004).

We therefore suggest, also considering our discussion of Sect. 5, that the processes for the heating and emission of chromospheric basal flux stars are largely attributable to the dissipation of mechanical energy. This form of energy is inherent in any star and shows little variability with time (except on stellar evolutionary time-scales). As its physical manifestation, acoustic waves and turbulent motions have been suggested as a candidate mechanism long time ago (e.g., Narain & Ulmschneider 1990). In combination they might also explain or contribute (in an appropriate 3-D implementation) to the spectroscopically derived near-sonic (or apparently even supersonic) turbulent velocities revealed by chromospheric line profiles.

The dissipation of a form of non-magnetic, supposedly acoustic wave energy deposited in the turbulent chromosphere, agrees with the refined empirical relationship, which we obtained for the basal flux including its dependence on the stellar effective temperature. Different approaches to derive the surface fluxes and the values for the effective temper-

atures yielded no significant differences (i.e., no more than 1σ of the involved statistical parameters).

In that sense, we can also confirm that our results agree with previously attained hydrodynamic chromosphere models, also noting that the mechanical energy deposited in the Mg II $h+k$ line formation regions vary very little with gravity. In fact, within the uncertainties, our relation renders the same basal flux even over four orders of magnitude as has been attained for MS stars. Still, a small contribution to the basal flux from heating processes related to some permanent, weak magnetic carpet cannot entirely be ruled out since the empirical basal flux appears to be slightly higher (by about its inherent uncertainty) than the fluxes suggested by previous acoustic heating models. In fact, it has been argued that magnetic fields might also contribute to balancing the basal emission flux (Judge & Carpenter 1998), although more detailed studies are still needed to further investigate this claim.

It is also noteworthy that the upward propagating mechanical flux and energy required for driving a cool wind emerging from the outer chromosphere is about an order of magnitude smaller than the total mechanical turn-over of the turbulent chromosphere in the above mentioned models. Hence, it may be possible for a turbulent giant chromosphere to divert such a small fraction of its mechanical flux to drive a cool star wind. It is intriguing that both the basal flux and a matching wind energy input show about the same dependency on T_{eff} (by a power of 7.5, as assumed by Schröder & Cuntz 2005), and neither seems to depend considerably on gravity. An extended giant chromosphere definitely assists a cool star wind in another aspect: Mass loss emerging from the outer chromosphere requires a lot less energy input compared to a wind originating directly from the stellar photosphere due to the reduction in the required amount of potential energy. These two arguments strongly support the idea that the mechanical energy reservoir of the chromosphere, as probed by the basal flux, also nurtures the wind energy input, possibly associated with weak magnetic fields.

Updated models based on structured red giant winds have meanwhile been presented by Suzuki (2007). He attributes the occurrence of mass loss to the action of Alfvén waves, excited by surface convection, which travel outward while dissipating via non-linear processes to accelerate and heat the stellar winds; see, e.g., Hartmann & MacGregor (1980), Hartmann & Avrett (1984) and Airapetian et al. (2000) for previous models of mass loss concerning low-gravity stars invoking Alfvén waves. In case of hybrid stars, Suzuki (2007) advocates the existence of hot bubbles, which are the source of the observed UV/soft X-ray emission. Clearly, in the framework of cool giant chromospheres and winds, it appears that there might be an intricate interplay of different processes operating on different scales which are responsible for producing the observed phenomena and features.

ACKNOWLEDGMENTS

This work has been supported by the Mexican Science Foundation CONACyT under their postgrad-student grant program and by CONACyT grant No. 80804 (CB-2007). Furthermore, we are very grateful for the on-line availability

of the IUE final data archive at STScI, without which this study would not have been possible.

REFERENCES

- Airapetian V. S., Ofman L., Robinson R. D., Carpenter K., Davila J., 2000, *ApJ*, 528, 965
- Ayres T. R., 1979, *ApJ*, 228, 509
- Ayres T. R., Brown A., Harper G. M., 2003, *ApJ*, 598, 610
- Baliunas S. L. et al., 1995, *ApJ*, 438, 269
- Barnes T. G., Evans D. S., Moffett T. J., 1978, *MNRAS*, 183, 285
- Buchholz B., Ulmschneider P., Cuntz M., 1998, *ApJ*, 494, 700
- Buzzoni A., Patelli L., Bellazzini M., Fusi Pecci F., Oliva E., 2010, *MNRAS*, 403, 1592
- Cardini D., 2005, *A&A*, 430, 303
- Charbonneau P., Schrijver C. J., MacGregor K. B., 1997, in Jokipii J.R., Sonett C.P., Giampapa M.S., eds, *Cosmic Winds and the Heliosphere*, Univ. of Arizona Press, Tucson, p. 677
- Cox A. N., 2001, *Allen's Astrophysical Quantities*, 4th Ed., Springer, New York
- Cuntz M., 1990, *ApJ*, 353, 255
- Cuntz M., Rammacher W., Ulmschneider P., 1994, *ApJ*, 432, 690
- Cuntz M., Ulmschneider P., Musielak Z. E., 1998, *ApJ*, 493, L117
- Cuntz M., Rammacher W., Ulmschneider P., Musielak Z. E., Saar S. H., 1999, *ApJ*, 522, 1053
- Dupree A. K., Hartmann L., Smith G. H., 1990, *ApJ*, 353, 623
- Fawzy D., Ulmschneider P., Stępień K., Musielak Z. E., Rammacher W., 2002, *A&A*, 386, 983
- Gray D. F., 1991, in Catalano S., Stauffer J.R., eds, *Angular Momentum Evolution of Young Stars*, Kluwer, Dordrecht, p. 183
- Hartmann L., Avrett E. H., 1984, *ApJ*, 284, 238
- Hartmann L., MacGregor K. B., 1980, *ApJ*, 242, 260
- Holzer T. E., MacGregor K. B., 1985, in Morris M., Zuckerman B., eds, *Mass Loss from Red Giants*, Reidel, Dordrecht, p. 229
- Judge P. G., 1990, *ApJ*, 348, 279
- Judge P. G., Carpenter K. G., 1998, *ApJ*, 494, 828
- Judge P. G., Cuntz M., 1993, *ApJ*, 409, 776
- Judge P. G., Stencel R. E., 1991, *ApJ*, 371, 357
- Linsky J. L., Ayres T. R., 1978, *ApJ*, 220, 619
- Montgomery D. C., Peck E. A., Vining G. G., 2006, *Introduction to Linear Regression Analysis*, 4th edn., Wiley-Interscience, Hoboken, NJ
- Musielak Z. E., 2004, in Dupree A.K., Benz A.O., eds, *IAU Symp. 219, Stars as Suns: Activity, Evolution and Planets*, Astron. Soc. Pac., San Francisco, p. 437
- Musielak Z. E., Rosner R., 1988, *ApJ*, 329, 376
- Narain U., Ulmschneider P., 1990, *Space Science Reviews*, 54, 377
- Nichols J. S., 1998, *ESA-SP*, 413, 671
- Nichols J. S., Linsky J. L., 1996, *AJ*, 111, 517
- Oranje B. J., Zwaan C., 1985, *A&A*, 147, 265
- Oranje B. J., Zwaan C., Middelkoop F., 1982, *A&A*, 110, 30
- Pasquini L., de Medeiros J. R., Girardi L., 2000, *A&A*, 361, 1011
- Peterson R. C., Schrijver C. J., 1997, *ApJ*, 480, L47
- Press W. H., Flannery B. P., Teukolsky S. A., Vetterling W. T., 1986, *Numerical Recipes*, Cambridge Univ. Press, Cambridge, UK
- Reimers D., 1977, *A&A*, 61, 217; Erratum, 67, 161 [1978]
- Rutten R. G. M., Pylyser E., 1988, *A&A*, 191, 227
- Rutten R. G. M., Schrijver C. J., Lemmens A. F. P., Zwaan C., 1991, *A&A*, 252, 203
- Schrijver C. J., 1987, *A&A*, 172, 111
- Schrijver C. J., 1993, in Weiss W.W., Baglin A., eds, *IAU Coll. 137, Inside the Stars*, Astron. Soc. Pac., San Francisco, Vol. 40, p. 591
- Schrijver C. J., Pols O. R., 1993, *A&A*, 278, 51
- Schröder K.-P., Cuntz M., 2005, *ApJ*, 630, L73
- Schröder K.-P., Cuntz M., 2007, *A&A*, 465, 593
- Schröder K.-P., Hünsch M., Schmitt J. H. M. M., 1998, *A&A*, 335, 591
- Simon T., Drake S. A., 1989, *ApJ*, 346, 303
- Stencel R. E., Linsky J. L., Mullan D. J., Basri G. S., Worden S. P., 1980, *ApJS*, 44, 383
- Strassmeier K. G., Handler G., Paunzen E., Rauth M., 1994, *A&A*, 281, 855
- Sutmann G., Cuntz M., 1995, *ApJ*, 442, L61
- Suzuki T. K., 2007, *ApJ*, 659, 1592
- Theurer J., Ulmschneider P. & Kalkofen W., 1997, *A&A*, 324, 717
- Ulmschneider P., 1988, *A&A*, 197, 223
- Ulmschneider P., 1989, *A&A*, 222, 171
- Ulmschneider P., 1991, in Ulmschneider P., Priest E.R., Rosner R., eds, *Mechanisms of Chromospheric and Coronal Heating*, Springer, Berlin, p. 328
- Vilhu O. & Walter F. M., 1987, *ApJ*, 321, 958
- Wedemeyer S., Freytag B., Steffen M., Ludwig H.-G. & Holweber H., 2004, *A&A*, 414, 1121
- Whittet D. C. B., van Breda I. G., 1978, *A&A*, 66, 57